ChemComm

COMMUNICATION

View Article Online
View Journal | View Issue

Cite this: *Chem. Commun.*, 2019, **55**, 10611

Received 22nd June 2019,
Accepted 1st August 2019

DOI: 10.1039/c9cc04800f

rsc.li/chemcomm

Excited-state effects on magnetic properties of U(III) and U(IV) pyrazolylborate complexes†

Robert F. Higgins, ‡[a] Caleb J. Tatebe,[b] Suzanne C. Bart[b] and Matthew P. Shores *[a]

For a family of uranium pyrazolylborate complexes, we observe correlations between excited-state mixing and slow relaxation of magnetization for U(III) complexes, and U···B distances in U(IV) complexes.

Understanding how to control the magnetic properties of paramagnetic molecules is important to applications such as magnetic resonance[1] and spintronics.[2] Electronic structure tuning, where excited states can govern a critical role in ground-state magnetic properties, is a key method in the design of new materials for these applications. The excited-state influence is challenging to control synthetically: excited-state mixing can enhance dynamic magnetic properties of transition metal complexes,[3] whereas such mixing can be detrimental for lanthanides.[4] Actinide electronic structures are dissimilar to both 3d- and 4f-species concerning isolated ground-states and magnetic anisotropy. Specifically, excited-state effects on ground-state magnetic properties, including magnetic anisotropy and temperature-independent paramagnetism, are poorly understood for the actinides.[5,6] Therefore, determining the potential influence of excited states on magnetic properties in 5f elements is of pressing interest.[7–9]

Related recent reports have helped establish applicable trends between reactivity and electronic properties of uranium complexes/clusters.[10–16] While this research has been essential to advance our knowledge of these unique molecular species, the role(s) of small energy phenomena, including the impact of excited states on the magnetic properties of actinides, is an underrepresented aspect of current research. Kindra and Evans recently published a comprehensive review on the magnetic properties and susceptibility values for >500 actinide complexes, which highlights the value in assigning accurate oxidation states and other properties;[5] simultaneously, it accentuates the difficulty in analysing magnetic trends for these unique molecular species.[5]

A systematic study of the variation in excited-state mixing for uranium(III/IV) complexes with similar ligand fields is currently lacking; however, given our initial findings on a family of mono- and dinuclear bis-Tp*U complexes (Tp* = hydro-tris-(3,5-dimethylpyrazolyl)borate),[17] and the rich history of UTp*$_2$ complexes more generally,[18,19] we aimed to further explore the magnetic properties of this family. Herein, we have analysed the excited-state effects on magnetic properties for a series of mono- and dinuclear UTp*$_2$ complexes and found relationships between ligand bonding and magnetic properties (dynamic and static) across two uranium oxidation states.

The five U(III) and four U(IV) complexes that are magnetically characterised and analysed are shown in Scheme 1. The collected magnetic properties, including field-dependent magnetisation data (Fig. S7–S9, ESI†), corroborate our initial assignments for the oxidation states of each complex.[5,20–22] Furthermore, no evidence of magnetic exchange coupling was observed for the dinuclear complexes [(Tp*$_2$U)$_2$(*p*-DIB)], [(Tp*$_2$U)$_2$(*m*-DIB)], [(Tp*$_2$U)$_2$-*p*-DEB] and [(Tp*$_2$U)$_2$-*m*-DEB] (DIB = diimidobenzene, DEB = diethynylbenzene), which indicated that the uranium ions could be treated individually.

Our efforts turned to investigating the contributions of excited states in the magnetic properties of these complexes, as recently described by Chilton and Liddle for the chalcogenide series in [{U(N(CH$_2$CH$_2$NSi^{i}Pr$_3$)$_3$)}$_2$(μ-S/Se/Te)].[23] In eqn (1) (shown below),[23]

$$\hat{H} = \sum_{k=2,4,6} \sum_{q=-k}^{k} B_k^q \hat{O}_k^q + \mu_B g_J \hat{J} \cdot \vec{B} \qquad (1)$$

the fitted parameters used by Chilton and Liddle included the axial crystal field (B_2^0); orbital reduction parameter (k), a measure of covalency; and the Lande (g_J) factor, the correlation between magnetic susceptibility and angular momentum for a given system. This report indicated that subtle inflection points in χ_M *vs.* T data at lower temperatures, ~20–30 K, derived from

[a] *Department of Chemistry, Colorado State University, Fort Collins, Colorado 80523, USA. E-mail: matthew.shores@colostate.edu*
[b] *H. C. Brown Laboratory, Department of Chemistry, Purdue University, West Lafayette, Indiana 47907, USA*

† Electronic supplementary information (ESI) available: Additional magnetic characterizations. See DOI: 10.1039/c9cc04800f

‡ Current address: P. Roy and Diana T. Vagelos Laboratories, Department of Chemistry, University of Pennsylvania, Philadelphia, Pennsylvania 19104, USA.

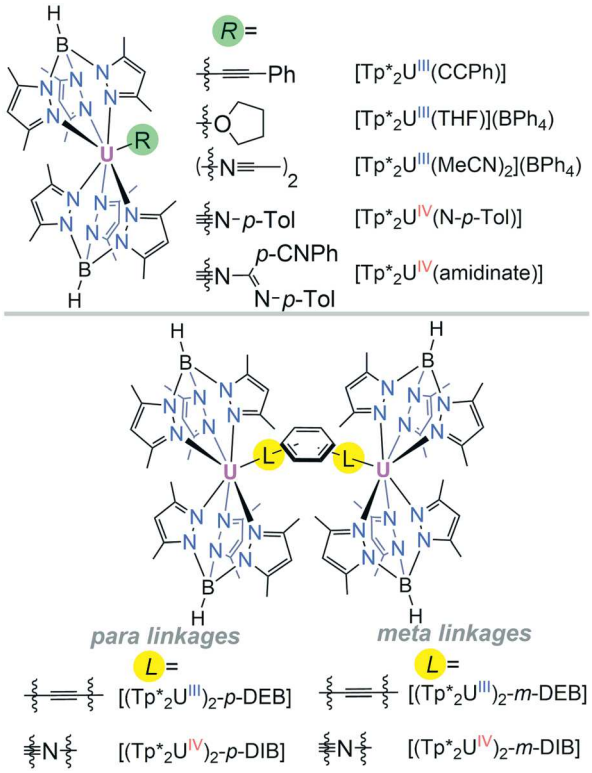

Scheme 1 Line-bond representations of molecules of interest in this study (DIB = diimidobenzene, DEB = diethynylbenzene).

crystal-field effects instead of the traditional explanation of magnetic exchange coupling.

Analyses of the χ_M *vs.* T data for tetravalent [Tp*$_2$U = N-*p*-Tol], [(Tp*$_2$U)$_2$(*p*-DIB)], [(Tp*$_2$U)$_2$(*m*-DIB)], and [Tp*$_2$U(amidinate)] indicate that these effects are likely present in the UTp*$_2$ framework studied here (Fig. 1). Notably, a subtle plateau in the χ_M values from about 20–30 K was observed to varying degrees for these complexes suggestive of different crystal-field effects for each

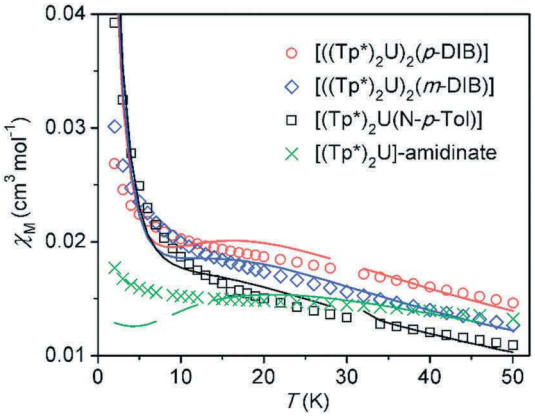

Fig. 1 Temperature dependence of the magnetic susceptibility for [Tp*$_2$U = N-*p*-Tol], [(Tp*$_2$U)$_2$-*p*-DIB], [(Tp*$_2$U)$_2$-*m*-DIB] and [Tp*$_2$U(amidinate)] per U-atom, where the 2–50 K data points are fit (lines) assuming J = 4, using the program PHI.[24] Inset: Zoom of the low temperature fits. Individual plots representing the fits with χ_M, $\chi_M T$, χ_M^{-1} and μ_{eff} *vs.* T are available in the ESI.†

Table 1 Parameters for the magnetic fits for [Tp*$_2$U = N-*p*-Tol], [(Tp*$_2$U)$_2$-*p*-DIB], [(Tp*$_2$U)$_2$-*m*-DIB] and [Tp*$_2$U(amidinate)] using the program PHI[23]

Complex	B_2^0 (cm^{-1})	k	g_J	R^2	U···B distance (Å)
[Tp*$_2$U = N-*p*-Tol]	1.22	0.760	1.00	99.992	3.70(1)
[(Tp*$_2$U)$_2$-*p*-DIB]	1.38	0.798	1.18	99.993	3.69(1)
[(Tp*$_2$U)$_2$-*m*-DIB]	13.2	0.831	1.33	99.990	3.67(1)
[Tp*$_2$U]-amidinate	31.1	0.805	1.37	99.985	3.63(1)

complex. To probe these crystal-field parameters, the data are fit in a similar fashion to Chilton and Liddle's method,[23,24] with J = 4 for all U(IV) ions; the results of these fits are shown in Table 1. The focus is placed on the low temperature region (2–50 K) since crystal-field effects will be most pronounced at lower temperatures. The fits are consistent with other U(IV) complexes with regard to their orbital reduction (k) and Landé (g_J) parameters.[23,25] Unsurprisingly, all four of these complexes show smaller k values (where k = 1 is fully ionic) compared to previously reported bridging U–chalcogenide–U species, consistent with the expectation that metal-imido bonds should display more covalent behaviour.

Interestingly, the crystal-field parameter (B_2^0) differs greatly when [(Tp*$_2$U)$_2$-*m*-DIB] is compared to [(Tp*$_2$U)$_2$-*p*-DIB] and [Tp*$_2$U = N-*p*-Tol] (Table 1). These results are interesting considering the orbital splitting is expected to be similar given the geometries and ligand fields about the individual U atoms. Compound [(Tp*$_2$U)$_2$-*m*-DIB] shows an average U···B distance of 3.66(1) Å, whereas compounds [(Tp*$_2$U)$_2$-*p*-DIB] and [Tp*$_2$U = N-*p*-Tol] display U···B distances of 3.70(1) and 3.69(1) Å, respectively. The shorter U···B distances for [(Tp*$_2$U)$_2$-*m*-DIB] compress the Tp* ligands closer to the U centre, which is expected to increase the energies of unfilled σ* symmetric frontier orbitals, which in turn increases the B_2^0 value. To further validate these excited-state energies for [(Tp*$_2$U)$_2$-*p*-DIB] and [(Tp*$_2$U)$_2$-*m*-DIB], another complex, [Tp*$_2$U(amidinate)], was measured and analysed. Its molecular structure indicates an average U···B distance of 3.63(1) Å, expanding the range of U···B distances for this family of U-imido complexes.[17] Interestingly, fitting the magnetic susceptibility data for [Tp*$_2$U(amidinate)] gives the largest B_2^0 value of the family, and provides a robust relationship between crystal-field splitting values and the U···B distances (Fig. 2). Therefore, we hypothesize that to increase B_2^0 values and potentially perturb other crystal-field phenomena in UTp*$_2$ complexes, the most straightforward manner appears to involve decreasing the U···B distance, which could be accomplished by using less-donating imido or imido-like ancillary ligands, such as ureates or guanidinates. As a note, no distinct trend was observed between crystal field parameters obtained from the fits of the magnetic data and other crystallographic parameters (*e.g.*, U–N distance, Table S1, ESI†).

Whereas U(IV) (f^2 electronic configuration) complexes consistently show a singlet ground state, U(III) (f^3 electronic configuration) ions are interesting for their properties pertaining to slow magnetic relaxation.[8,26,27] Specifically, many U(III) complexes

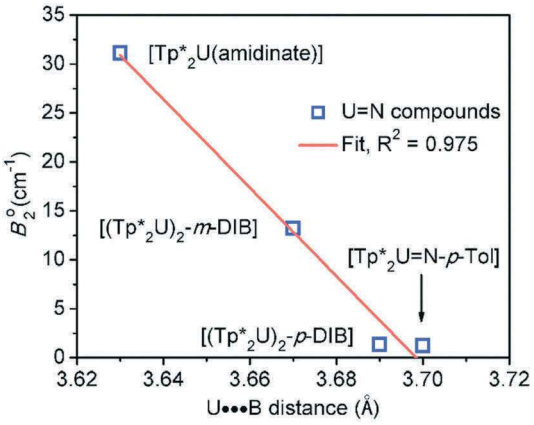

Fig. 2 Correlation between obtained B_2^0 values and U···B distances.

with field-induced slow relaxation properties bear a pyrazolyl-borate ligand set.[12,28–30] Here, dynamic magnetic data collected for the dinuclear UTp*$_2$ complexes indicate that [(Tp*$_2$U)$_2$-*p*-DEB] and [(Tp*$_2$U)$_2$-*m*-DEB] likely display magnetic relaxation at high frequencies (Fig. S14 and S16, ESI†); however, due to the limits of our instrumentation and the fast rate of relaxation, relaxation barriers and lifetimes are not quantifiable. Interestingly, all three mononuclear complexes, [Tp*$_2$UCCPh], [Tp*$_2$U(THF)](BPh$_4$) and [Tp*$_2$U(MeCN)$_2$](BPh$_4$), display magnetic relaxation that is slow

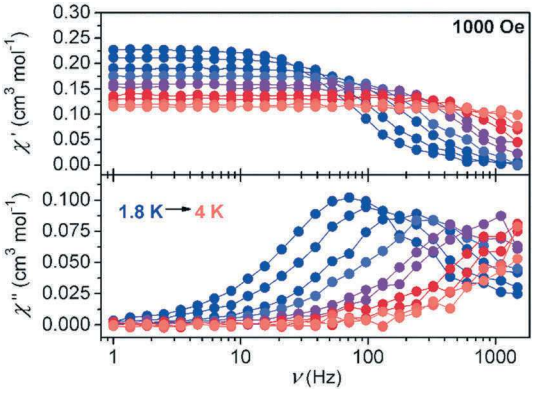

Fig. 3 Variable temperature in- (top) and out-of-phase (bottom) magnetic susceptibility data for [Tp*$_2$U(MeCN)$_2$](BPh$_4$) collected with an oscillating ac field of 4 Oe and an applied dc field of 1000 Oe.

enough for us to characterise (Fig. 3). While none of these complexes display zero-field relaxation at the frequency range measured, each shows field-induced magnetic relaxation that is optimised at applied dc fields of 500 Oe ([Tp*$_2$U(THF)](BPh$_4$)) and 1000 Oe ([Tp*$_2$UCCPh] and [Tp*$_2$U(MeCN)$_2$](BPh$_4$), Fig. S18–S27, ESI†). Fitting these data to the Arrhenius equation ($\tau = \tau_0 \exp(U_{eff} k_B^{-1} T^{-1})$) – for consistency with previously reported data – gives lifetimes and barriers that compare well to literature-precedented mononuclear U(III) complexes (Table 2 and Fig. S28, ESI†).[12,28–32] These pathways seem to include relaxation through mainly Raman processes but also include some Orbach contributions for [Tp*$_2$U(THF)](BPh$_4$), [Tp*$_2$UCCPh] and [Tp*$_2$U(MeCN)$_2$](BPh$_4$) (Fig. S28, ESI†). Orbach processes are extremely uncommon in U(III) single molecule magnets,[8] but nonetheless appear to be significant contributors in these systems. Notwithstanding, these data were also fit to a Raman expression, $\tau^{-1} = CT^n$, where C and n are the Raman coefficient and exponent, respectively, and are available in the ESI,† Fig. S29.

The most common cause for decreased magnetisation lifetimes and/or quantum tunnelling mechanisms for SMMs is dipolar interactions; this is especially prevalent in previously characterised U(III) complexes.[8] Interestingly, the closest intermolecular U···U distances are long in our complexes (9.064(4)–10.636(7) Å), as well as a lack of H-bonding and π-stacking pathways (Table S2, ESI†),[19,30] suggesting that the magnetic properties of these UTp*$_2$ complexes are unique.

Further, no clear trend is apparent for average U···B distances of these U(III) complexes, dissimilar to the U(IV) species (Table S2, ESI†). Charge density (*e.g.*, electrostatics) also does not appear to be a major factor as no obvious trend is observable when comparing cation/anion pairs and neutral complexes. These UTp*$_2$ species seem relatively unperturbed by coordination number since ligation to one or two ancillary groups does not generate an obvious trend for these species. Straightforward crystal-field approximations also fail to give a noticeable trend: an analysis of the nephelauxetic series suggests that [(Tp*)$_2$U(I)] and [(Tp*)$_2$U(CCPh)] should show similar properties, which is not experimentally observed.[33] As a first approximation, it might be expected that [Tp*$_2$U(THF)](BPh$_4$) and [Tp*$_2$U(MeCN)$_2$](BPh$_4$) would show similar properties that diverge from [Tp*$_2$UCCPh] based on differences in ligand field strength. Comparison to other Tp*$_2$U complexes suggests that simple ligand field arguments

Table 2 Selected magnetic properties acquired from fits using the program PHI[24] for some pyrazolylborate-containing U(III) complexes

Complex	τ_0 (1×10^{-6} s)	U_{eff} (cm^{-1})	g_J	B_2^0 (cm^{-1})	k	D (cm^{-1})
[Tp*$_2$U(I)][18,26]	0.18	21.0	0.539	17.1	0.811	−16.9
[Tp*$_2$U(bpy)](I)[27]	0.14	18.2	0.337	14.7	0.850	−22.4
[U(BPz$_2$H$_2$)$_3$][12]	1.2	8	0.426	5.5	0.731	−24.1
[(Tp*$_2$U)$_2$-*p*-DEB]	—	—	0.575	***19.7***	0.816	−20.7
[(Tp*$_2$U)$_2$-*m*-DEB]	—	—	0.690	***28.7***	0.862	−14.4
[Tp*$_2$UCCPh]	2.1	6.81	0.507	15.7	0.756	−15.6
[Tp*$_2$U(THF)](BPh$_4$)	4.3	9.00	0.516	16.1	0.869	−9.8
[Tp*$_2$U(MeCN)$_2$](BPh$_4$)	4.0	8.36	0.624	9.7	0.896	−16.9

(— = not observed).

cannot be used to rationalise the dynamic magnetic properties of these complexes (Table 2).[29,30]

An alternative approach to determine crystal-field parameters is fitting magnetic susceptibility data, akin to what was applied to the U(IV) complexes (*vide supra*).[23] For the U(III) complexes, the fits indicate no clear trend between the dynamic magnetic properties and the parameters g_J, k or D; however, the B_2^0 term is largest for [$(Tp^*_2U)_2$-*p*-DEB] and [$(Tp^*_2U)_2$-*m*-DEB] when compared to all other magnetically characterized UTp^*_2 species, including various literature examples (Table 2 and Fig. S11–S13, ESI†). Potentially more important, the B_2^0 (and D) values acquired from these fits for [$Tp^*_2U(I)$], [$Tp^*_2U(bpy)$](I) and [$U(BPz_2H_2)_3$] are in qualitative agreement with computations performed using the SO-CASPT2 method, supporting the validity of these fits.[30] A note of caution should be taken since B_2^0 and D both describe axial anisotropic distortions as different parameters in the applied Hamiltonian; however, both terms were required to fit the lower temperature (<20 K) data.

These results suggest that the B_2^0 term dictates the dynamics of slow magnetic-relaxation for U(III) complexes. Specifically, a decrease in excited-state mixing for [$(Tp^*_2U)_2$-*p*-DEB] and [$(Tp^*_2U)_2$-*m*-DEB] increases the possibility for quantum tunnelling of magnetisation and/or decreases relaxation lifetimes. This is significant as it has been previously reported that U(III) complexes show slow magnetic relaxation, regardless of ligand field or coordination geometry.[31] A moderate correlation between increased excited-state mixing (smaller B_2^0 values) and extension of the attempt times (τ_0) was also observed (Table 2). These results give an alternative design approach for enhancing dynamic magnetic properties in U(III) complexes,[8] as the trends determined herein oppose the design guidelines for lanthanide counterparts, where isolation of a pure ground state enhances dynamic magnetic properties for 4f species.[34]

In conclusion, we report experimental evidence for a new design strategy of U(III) molecular magnets by decreasing U–Tp* distances through electronic tuning of ancillary ligands to affect magnetic relaxation through changes in the excited-state occupation of the uranium compounds. Importantly, these features are consistent across different oxidation states of U-complexes, highlighting its potential impact.

RFH and MPS thank the NSF (CHE-1363274 and CHE-1800554) for support of magnetometry measurements at Colorado State University. CJT and SCB thank the NSF for supporting this work (CHE-1665170, SCB). We also acknowledge Professors Jeffrey R. Long (UC Berkeley) and Joseph M. Zadrozny (CSU) for constructive conversations.

Conflicts of interest

There are no conflicts to declare.

Notes and references

1 D. V. Hingorani, A. S. Bernstein and M. D. Pagel, *Contrast Media Mol. Imaging*, 2015, **10**, 245–265.
2 L. Bogani and W. Wernsdorfer, *Nat. Mater.*, 2008, **7**, 179–186.
3 J. M. Frost, K. L. M. Harriman and M. Murugesu, *Chem. Sci.*, 2016, **7**, 2470–2491.
4 J. D. Rinehart and J. R. Long, *Chem. Sci.*, 2011, **2**, 2078–2085.
5 D. R. Kindra and W. J. Evans, *Chem. Rev.*, 2014, **114**, 8865–8882.
6 L. R. Morss, N. M. Edelstein and J. Fuger, *The chemistry of the actinide and transactinide elements*, Springer, Dordrecht, 4th edn, 2010.
7 S. T. Liddle, *Angew. Chem., Int. Ed.*, 2015, **54**, 8604–8641.
8 K. R. Meihaus and J. R. Long, *Dalton Trans.*, 2015, **44**, 2517–2528.
9 S. T. Liddle and J. van Slageren, *Chem. Soc. Rev.*, 2015, **44**, 6655–6669.
10 P. L. Arnold, G. M. Jones, S. O. Odoh, G. Schreckenbach, N. Magnani and J. B. Love, *Nat. Chem.*, 2012, **4**, 221–227.
11 D. P. Mills, F. Moro, J. McMaster, J. van Slageren, W. Lewis, A. J. Blake and S. T. Liddle, *Nat. Chem.*, 2011, **3**, 454–460.
12 J. D. Rinehart and J. R. Long, *J. Am. Chem. Soc.*, 2009, **131**, 12558–12559.
13 M. Falcone, L. Chatelain, R. Scopelliti, I. Zivkovic and M. Mazzanti, *Nature*, 2017, **547**, 332–335.
14 V. Mougel, L. Chatelain, J. Pecaut, R. Caciuffo, E. Colineau, J. C. Griveau and M. Mazzanti, *Nat. Chem.*, 2012, **4**, 1011–1017.
15 D. P. Halter, F. W. Heinemann, L. Maron and K. Meyer, *Nat. Chem.*, 2018, **10**, 259–267.
16 S. A. Johnson, R. F. Higgins, M. M. Abu-Omar, M. P. Shores and S. C. Bart, *Organometallics*, 2017, **36**, 3491–3497.
17 C. J. Tatebe, J. J. Kiernicki, R. F. Higgins, R. J. Ward, S. N. Natoli, J. Langford, C. L. Clark, M. Zeller, P. Wenthold, M. P. Shores, J. R. Walensky and S. C. Bart, *Organometallics*, 2019, **38**, 1031–1040.
18 R. McDonald, Y. M. Sun, J. Takats, V. W. Day and T. A. Eberspracher, *J. Alloys Compd.*, 1994, **213**, 8–10.
19 Y. M. Sun, R. McDonald, J. Takats, V. W. Day and T. A. Eberspacher, *Inorg. Chem.*, 1994, **33**, 4433–4434.
20 E. J. Schelter, J. M. Veauthier, C. R. Graves, K. D. John, B. L. Scott, J. D. Thompson, J. A. Pool-Davis-Tournear, D. E. Morris and J. L. Kiplinger, *Chem. – Eur. J.*, 2008, **14**, 7782–7790.
21 E. J. Schelter, R. L. Wu, B. L. Scott, J. D. Thompson, T. Cantat, K. D. John, E. R. Batista, D. E. Morris and J. L. Kiplinger, *Inorg. Chem.*, 2010, **49**, 924–933.
22 J. J. Le Roy, S. I. Gorelsky, I. Korobkov and M. Murugesu, *Organometallics*, 2015, **34**, 1415–1418.
23 B. M. Gardner, D. M. King, F. Tuna, A. J. Wooles, N. F. Chilton and S. T. Liddle, *Chem. Sci.*, 2017, **8**, 6207–6217.
24 N. F. Chilton, R. P. Anderson, L. D. Turner, A. Soncini and K. S. Murray, *J. Comput. Chem.*, 2013, **34**, 1164–1175.
25 D. M. King, P. A. Cleaves, A. J. Wooles, B. M. Gardner, N. F. Chilton, F. Tuna, W. Lewis, E. J. L. McInnes and S. T. Liddle, *Nat. Commun.*, 2016, **7**, 13773.
26 F.-S. Guo, Y.-C. Chen, M.-L. Tong, A. Mansikkamäki and R. A. Layfield, *Angew. Chem., Int. Ed.*, 2019, **58**, 10163–10167.
27 S. Dey, G. Velmurugan and G. Rajaraman, *Dalton Trans.*, 2019, **48**, 8976–8988.
28 J. D. Rinehart, K. R. Meihaus and J. R. Long, *J. Am. Chem. Soc.*, 2010, **132**, 7572–7573.
29 M. A. Antunes, L. C. J. Pereira, I. C. Santos, M. Mazzanti, J. Marçalo and M. Almeida, *Inorg. Chem.*, 2011, **50**, 9915–9917.
30 J. T. Coutinho, M. A. Antunes, L. C. J. Pereira, H. Bolvin, J. Marçalo, M. Mazzanti and M. Almeida, *Dalton Trans.*, 2012, **41**, 13568–13571.
31 F. Moro, D. P. Mills, S. T. Liddle and J. van Slageren, *Angew. Chem., Int. Ed.*, 2013, **52**, 3430–3433.
32 J. D. Rinehart and J. R. Long, *Dalton Trans.*, 2012, **41**, 13572–13574.
33 B. N. Figgis and M. A. Hitchman, *Ligand field theory and its applications*, Wiley-VCH, New York, 2000.
34 R. A. Layfield, *Organometallics*, 2014, **33**, 1084–1099.

